Synchronization of Periodical Cicada Emergences

Frank C. Hoppensteadt, Joseph B. Keller

Science, New Series, Volume 194, Issue 4262 (Oct. 15, 1976), 335-337.

Stable URL:
http://links.jstor.org/sici?sici=0036-8075%2819761015%293%3A194%3A4262%3C335%3ASOPCE%3E2.0.CO%3B2-L

ments coding for the P proteins, nucleoprotein, membrane protein, and nonstructural protein are derived from PR8 virus.

In order to identify which RNA of X-53 codes for hemagglutinin and which for neuraminidase, the RNA pattern of another recombinant derived from influenza A/PR/8/34 and A/NJ/11/76 virus was analyzed. Serologic analysis of this recombinant demonstrated that like X-53 it derived its hemagglutinin from A/NJ/11/76 virus but its neuraminidase was shown to be of PR8 virus origin. RNA analysis of this recombinant (Fig. 2, lane 1) reveals that it has derived only the fourth RNA segment from the "swine" virus (lanes 2 and 3). This demonstrates that, as is the case with PR8 virus, the fourth RNA of the swine virus codes for the hemagglutinin and the sixth RNA for neuraminidase.

Our finding that the high-yielding recombinant X-53 has derived six of its genes from the PR8 virus does not necessarily indicate that the high yield characteristic requires all six PR8-derived genes. In the course of genetic reassortment PR8 genes not related to enhanced replication may have been incorporated by chance into X-53. Alternatively, because the PR8 virus replicates much faster than the "swine" virus in the allantoic cavity of embryonated eggs, a greater number of PR8 genes is thus available for recombination and might have been incorporated into the genome of the recombinant including some not required for transfer of the high yield characteristic. A definitive answer to the question of how many and which genes are necessary for the transfer of the property of "good growth" to an influenza virus recombinant awaits further genetic analysis.

PETER PALESE
MARY B. RITCHEY
JEROME L. SCHULMAN
EDWIN D. KILBOURNE
Department of Microbiology, Mount Sinai School of Medicine of the City University of New York, New York 10029

References and Notes

1. The serotype of influenza viruses is determined by its surface proteins hemagglutinin (H) and neuraminidase (N). For review, see E. D. Kilbourne, in *The Influenza Viruses and Influenza*, E. D. Kilbourne, Ed. (Academic Press, New York, 1975), p. 1.
2. E. D. Kilbourne and J. S. Murphy, *J. Exp. Med.* **111**, 387 (1960); E. D. Kilbourne, *Bull. WHO* **41**, 643 (1969); J. L. Schulman, G. C. Schild, G. Schloer, J. Swanson, D. Bucher, *J. Infect. Dis.* **124**, 449 (1971); E. D. Kilbourne, *ibid.*, in press.
3. U.S. Department of Health, Education, and Welfare, *Morb. Mortal. Wkly. Rep.* **25**, 47 (1976).
4. P. Palese and J. L. Schulman, *J. Virol.* **17**, 876 (1976); J. L. Schulman and P. Palese, *ibid.*, in press; M. B. Ritchey, P. Palese, E. D. Kilbourne, *ibid.* **18**, 738 (1976); M. B. Ritchey, P. Palese, J. L. Schulman, *ibid.*, in press; P. Palese, M. B. Ritchey, J. L. Schulman, in preparation.
5. P. Palese and J. L. Schulman, *Proc. Natl. Acad. Sci. U.S.A.* **73**, 2142 (1976).
6. J. L. Sever, *J. Immunol.* **80**, 320 (102); E. D. Kilbourne, W. G. Laver, J. L. Schulman, R. G. Webster, *J. Virol.* **2**, 281 (1968).
7. We thank Ms. Marlene Lin, Ms. Kaye Leitzinger, and Ms. Barbara Pokorny for technical assistance. This work was supported by NIH grants AI-11823 and AI-09394 and NSF grant PCM-76-11066.

24 May 1976; revised 9 July 1976

Synchronization of Periodical Cicada Emergences

Abstract. *Synchronized insect emergences are shown to be a possible consequence of predation in the presence of a limited environmental carrying capacity through a mathematical model for cicada populations that includes these two features. Synchronized emergences, like those observed in 13- and 17-year cicadas, are predicted for insects with sufficiently long life-spans. Balanced solutions, in which comparable emergences occur each year, are found for insects having sufficiently short life-spans, such as 3-, 4-, and 7-year cicadas. For the values used here, synchronized emergences occur for insects with life-spans of 10 years or more, and balanced emergences occur for life-spans of fewer than 10 years.*

Thirteen-year cicadas, *Magicicada* spp., appear in large numbers every 13 years, but practically none appear in intervening years (*1*). Seventeen-year cicadas emerge according to a similar pattern but they can bear both 13-year and 17-year progeny (*2*). The synchronization yields a periodic birth rate that is analogous to population waves studied in demography (*3*). However, the extreme form of the cicada periodicity cannot be maintained without mechanisms other than the usual birth and death schedules.

It has been suggested that predation and environmental carrying capacity can act in combination to bring about this synchronization (*1*, *4*). We have shown that this is indeed possible by constructing and analyzing a model of a cicada population that incorporates a predation threshold (*5*) (or predator satiation) and a limited carrying capacity. This model produces many features of cicada populations, such as synchronized emergences for cicadas with sufficiently long life-spans. The synchronized emergence is a consequence of the two conflicting requirements imposed by the predation threshold and the limited carrying capacity of the environment. On the one hand, the number of progeny produced in any year must exceed the predation threshold or they will be eliminated. On the other hand, their number cannot exceed the carrying capacity minus the living progeny produced in earlier years (residual carrying capacity). These requirements can best be met by a synchronized population when the life-span is long enough. However, they can also be met by a population with a short life-span having the same rate of emergence each year.

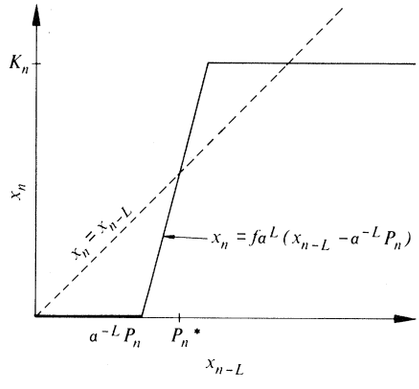

Fig. 1. The piecewise linear reproduction curve (Eq. 4), which determines the number (x_n) of nymphs becoming established underground in year n in terms of the number (x_{n-L}) in year $n - L$. This curve changes each year with the predation threshold (P_n) and the residual carrying capacity (K_n). The straight line $x_n = x_{n-L}$ is shown for reference.

Consider a species having a life-span of L years, with reproduction occurring in year L, followed by the death of the parents. Let x_{n-L} be the number of nymphs becoming established underground in year $n - L$. If α is their survival rate per year, then $x_{n-L}\alpha^L$ of them will survive L years and emerge as adults in year n. We assume that, when they emerge, predators will eliminate as many as P_n of them. There will be none left for mating if $x_{n-L}\alpha^L \leq P_n$; otherwise, there will be $x_{n-L}\alpha^L - P_n$ adults left. We denote this number by $(x_{n-L}\alpha^L - P_n)_+$ (*6*). If f is the number of hatched nymphs becoming established underground that each adult produces in a breeding period, then the total number of nymphs produced in year n is

$$H_n = f(x_{n-L}\alpha^L - P_n)_+ \quad (1)$$

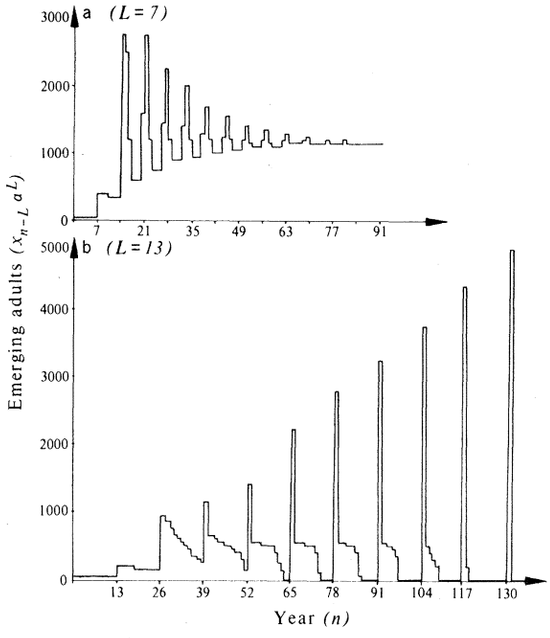

Fig. 2. Numerical solutions of the model (Eqs. 4 and 5) for (a) $L = 7$ and (b) $L = 13$. In both cases the parameter values are $K = 10{,}000$, $R = 0.95$, $\alpha = 0.95$, $A = 0.042$, and $f = 10$. The initial values were designed to reflect a hypothetical experiment where 100 nymphs are established at a site for L successive years, labeled $-L$, $-L + 1$, . . ., -1. In year 0, the first emergence occurs, and we set the predation threshold at 10, $P_0 = 10$. Therefore, in case $L = 7$, $x_i = 100$ for $i = -7, \ldots, -1$, and when $L = 13$, $x_i = 100$ for $i = -13, -12, \ldots, -1$. The number of emerging adults $x_{n-L}\alpha^L$ in year n is plotted for each year n. In (a), the emergences approach a balanced solution, and in (b), the synchronized state is reached after ten generations. Emergences are shown to the nearest 50.

We assume that all H_n nymphs enter the ground if the residual carrying capacity K_n can contain them, that is, if $K_n \geq H_n$. If not, only enough nymphs to fill the available space enter the ground. Thus x_n, the number of nymphs that become established in year n, is the minimum of H_n and K_n, that is, $x_n = \min(H_n, K_n)$. To find K_n, we let K be the total carrying capacity. Then the residual capacity is

$$K_n = K - \sum_{a=1}^{L-1} x_{n-a}\alpha^a \tag{2}$$

if this expression is positive, and otherwise K_n is zero. Thus,

$$K_n = \left(K - \sum_{a=1}^{L-1} x_{n-a}\alpha^a\right)_+ \tag{3}$$

Now we can write the equation $x_n = \min(H_n, K_n)$ in the explicit form

$$x_n = \min\left[f\left(x_{n-L}\alpha^L - P_n\right)_+ \left(K - \sum_{a=1}^{L-1} x_{n-a}\alpha^a\right)_+\right] \tag{4}$$

The predation threshold P_n accounts for all predators acting on the emergent population. We assume P_n to decrease from its previous level by a relaxation factor R and to increase an increment $Ax_{n-1-L}\alpha^L$ as a function of the size of the previous year's emergence. Thus we write

$$P_n = RP_{n-1} + Ax_{n-1-L}\alpha^L \tag{5}$$

Equations 4 and 5 constitute our model. They enable us to calculate the x_n and P_n successively for $n > L$ in terms of x_0, x_1, . . ., x_L and P_L (Fig. 1). The straight line $x_n = x_{n-L}$ intersects the reproduction curve at three points, the middle one of which is at

$$x_n = x_{n-L} = P_n^* \tag{6}$$

where

$$P_n^* = fP_n/(f\alpha^L - 1) \tag{7}$$

We call P_n^* the threshold of extinction since the progeny of year class n approach extinction if x_{n-L} falls below P_n^*. Furthermore, the whole population approaches extinction unless $f\alpha^L > 1$ and $R < 1$, which we assume to hold. If there is no emergence in year n, there is no emergence in any later year $n + NL$ with $N = 1, 2, \ldots$. In general, the reproduction curve changes from year to year as P_n and K_n change (7).

The solutions of Eqs. 4 and 5 behave differently for different parameter values and different initial conditions. In some cases, the progeny of all year classes become extinct, and in others, the solution is balanced and all years have identical emergences. In still other cases, the progeny of one specific year class approach the carrying capacity of the environment, and the progeny of all other year classes approach extinction. This is the synchronized solution that describes the periodical cicadas.

We shall not present an exhaustive analysis of these and the other possibilities. Instead we shall first find conditions that are necessary in order for a balanced solution to occur. Then we shall present the results of numerical computation, which show how a stable synchronized solution develops when no balanced solution is possible and how a balanced solution can develop when it is possible.

For a stable balanced solution to exist, all the x_n must be equal, and x_n must be given by the second term on the right side of Eq. 4. This yields

$$x_n = \frac{K(1 - \alpha)}{1 - \alpha^L} \tag{8}$$

Then Eq. 5 shows that P_n tends to the value

$$P_n = \frac{A\alpha^L x_n}{1 - R} \tag{9}$$

Furthermore, the condition that the first term on the right side of Eq. 4 exceed the second term yields

$$x_n > P_n^* = \frac{fP_n}{f\alpha^L - 1} \tag{10}$$

By using the limiting value of P_n in this inequality and canceling x_n, we are left with the condition

$$B \equiv \frac{Af\alpha^L}{(f\alpha^L - 1)(1 - R)} < 1 \tag{11}$$

This is a necessary condition for the existence of a stable balanced solution, and B is defined by this equation.

A synchronized solution is of the form $x_{NL} = K$ and $x_{NL+j} = 0$, $j = 1, \ldots, L - 1$. Then it follows that $P_{n+L} = P_n$, and so

$$P_{NL+j} = \frac{R^{j-1}KA\alpha^L}{1 - R^L}, \quad j = 1, \ldots, L \tag{12}$$

In order that this solution satisfy Eq. 4, it is necessary that $x_{NL} > P_{NL}^*$, which leads to

$$S \equiv \frac{Af\alpha^L R^{L-1}}{(f\alpha^L - 1)(1 - R^L)} < 1 \tag{13}$$

This relation, which defines S, is necessary for the existence of a synchronized solution.

From the definitions of B and S in Eqs. 11 and 13, it follows that $S < B$ for $L > 1$. Therefore, whenever $B < 1$, so that a balanced solution exists, $S < 1$ and a synchronized solution also exists. Similarly if $S > 1$, so that no synchronized solution exists, then $B > 1$ and no balanced solution exists either. But if $S < 1 < B$, then a synchronized but not a balanced solution exists. This is the case in which, starting with rather arbitrary initial values, the solution becomes synchronized.

We have calculated the solution of Eqs. 4 and 5 for a population with uniformly distributed initial emergences. With the parameter values chosen, $S < 1 < B$ for $L \geq 10$, and $S < B < 1$ for $2 \leq L \leq 9$. For $L = 11, 12, \ldots, 17$, the solution evolved into a synchronized solution, but for $L = 7$ it approached a balanced solution (Fig. 2).

In agreement with the model, cicadas with life-spans of 13 and 17 years have synchronized emergences, and those with life-spans of 3, 4, and 7 years have balanced emergences. However, this model and analysis do not explain why the life-span of the periodical cicadas should be 13 or 17 years or why changes in the life cycle, such as 4-year accelerations, occur.

FRANK C. HOPPENSTEADT
JOSEPH B. KELLER
Courant Institute of Mathematical Sciences, New York University, New York 10012

References and Notes

1. R. D. Alexander and T. E. Moore, *Univ. Mich. Mus. Zool. Misc. Publ. No. 121* (1962).
2. J. White and M. Lloyd, *Am. Midl. Nat.* **94**, 127 (1975).
3. H. Bernardelli showed that, in a species whose reproductive window is short compared with its life-span, the birth rate can be a periodic function of time [cited by P. H. Leslie, *Biometrika* **33**, 183 (1945)].
4. M. Lloyd and H. S. Dybas, *Evolution* **20**, 133 (1966); *ibid.*, p. 466.
5. C. S. Holling, *Annu. Rev. Ecol. Syst.* **4**, 1 (1973).
6. The notation $(y)_+$ denotes y if $y > 0$ and 0 if $y \leq 0$.
7. Our model leads to the piecewise linear reproduction curve in Fig. 1. It is similar to, but simpler than, those used in studying fisheries and other ecological systems, where they are referred to as depensatory-compensatory (d-c) curves [P. A. Larkin, R. F. Raleigh, N. J. Wilimovsky, *J. Fish. Res. Board Can.* **21**, 477 (1964); (*5*)]. In addition, in our model the curve changes at each generation. Results similar to the ones presented can be derived for more general d-c reproduction curves. For example, Eq. 4 can be replaced by $x_n = F(x_{n-L}; P_n, K_n)$ where F is a smooth function satisfying $F(x) < x$ for $0 < K_n < x < P_n^*$ and $F(x) > x$ for $0 < P_n^* < x < K_n$. Such a function is given by $F(x) = [x - x(P_n^* - x)\,(K_n - x)]_+$. The threshold of extinction P_n^* and the residual carrying capacity K_n can be defined as in the present model.
8. Supported in part by National Science Foundation grant NSF-MPS75-09837. We thank M. Lloyd and M. Levandowsky for their comments and suggestions.

9 January 1976; revised 7 May 1976

Variations in Writing Posture and Cerebral Organization

Abstract. *Two tachistoscopic tests of cerebral lateralization were administered to 73 subjects classified by handedness, sex, and hand orientation in writing. The results indicated that the direction of cerebral lateralization could be indexed from a subject's handedness and hand posture during writing. In subjects with a normal writing posture, the linguistically specialized hemisphere was contralateral to the dominant hand, and the visuospatially specialized hemisphere was ipsilateral; the reverse was true in subjects with an "inverted" hand position during writing. Females and subjects having an inverted hand posture manifested smaller degrees of lateral differentiation than males and subjects with a typical hand posture.*

In the vast majority of right-handed persons, the left cerebral hemisphere is specialized for language integration and the right hemisphere is specialized for mental imagery and the understanding of spatial relationships (*1*). The association between the linguistically dominant left hemisphere and the dominant right hand seems to derive from the fact that the left side of the brain is organized not only for language integration but also for the programming of sequential manual movements. Unilateral lesions of the left hemisphere produce ideational and ideomotor apraxias as well as aphasia and agraphia (*2*).

However, the understanding of the association between handedness and brain organization has been inadequate because of the complexity of the relationship between the brain and the hand in the left-handed. The left-handed population is heterogeneous with respect to the direction of lateral specialization; some 60 percent have language functions in the left hemisphere and visuospatial functions in the right, and about 40 percent have the opposite organization (*3*). In addition, some small fraction, probably less than 1 percent, of right-handed writers, have their main language functions in the right hemisphere and their visuospatial functions in the left (*4*). In left-handed writers with language functions in the left hemisphere or right-handed writers with language functions in the right hemisphere, control of the writing hand must be exercised either via the ipsilateral motor tracts, via commissural pathways, or, possibly, through both systems.

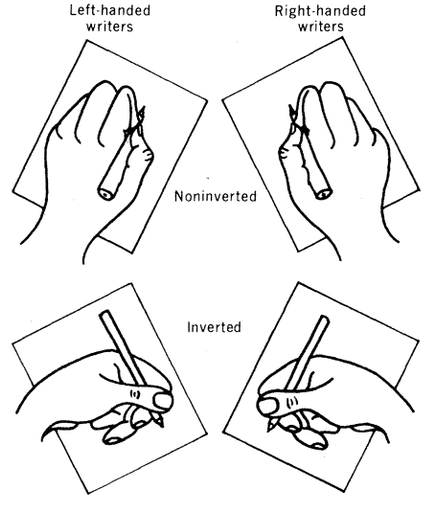

Fig. 1. Typical writing postures of dextrals and sinistrals who write with inverted and noninverted hand positions.

We now report a simple measurement which, in association with handedness, can reliably predict which hemisphere is predominantly linguistic and which primarily "spatial" in the left-handed and the occasional right-handed writer who is an exception to the normal relationship. Left-handed writers, in addition to being heterogeneous with respect to the direction of cerebral lateralization, also vary with respect to hand posture in writing. From our observations, more than 90 percent can be clearly classified as adopting either the "hooked" position, in which the hand lies above the line of writing, or the common right-handed position, in which the hand lies below the line of writing (Fig. 1). The hooked writing posture has been explained as a learned adaptation to the necessity of writing from left to right in our culture (*5*). Two observations make this interpretation unlikely. (i) We have observed several dextral writers who hold their hands above the line of writing in the inverted manner of a hooked left-handed writer. (ii) Writing in Hebrew proceeds from right to left, but in Israel, right-handed writers position their hands in the same way as Americans, but many left-handed Israelis display the hooked posture (*6*).

Results of a preliminary study by Levy and Mandel (*7, 8*) supported the hypothesis that writing position was related to cerebral dominance and indicated that the inverted position of left-handed writers was associated with an ipsilateral language hemisphere and the noninverted position with a contralateral language hemisphere. However, sources of noise in the data left other possible interpretations open.

We have now tested 73 subjects, all university undergraduates, for cerebral lateralization with two tachistoscopic tests, one measuring visuospatial dominance and one measuring language dominance. There were 24 right-handed writers with the noninverted position (RN), 24 left-handed writers with an inverted hand position (LI), 24 left-handed writers with the noninverted position (LN), and one right-handed writer with the inverted position (RI). Half of each group was male and half, female. Subject RI was a female. Hand position was classified according to two criteria: (i) whether the hand was held below (noninverted) or above (inverted) the line of writing, and (ii) whether the point of the pencil pointed toward the